

Dependence of interface conductivity on relevant physical parameters in polarized Fermi mixtures

N. Ebrahimian,^{1,*} M. Mehrafarin,^{1,†} and R. Afzali^{2,‡}

¹*Physics Department, Amirkabir University of Technology, Tehran 15914, Iran*

²*Physics Department, K.N. Toosi University of Technology, Tehran 15418, Iran*

Abstract

We consider a mass-asymmetric polarized Fermi system in the presence of Hartree-Fock (HF) potentials. We concentrate on the BCS regime with various interaction strengths and numerically obtain the allowed values of the chemical and HF potentials, as well as the mass ratio. The functional dependence of the heat conductivity of the N-SF interface on relevant physical parameters, namely the temperature, the mass ratio, and the interaction strength, is obtained. In particular, we show that the interface conductivity starts to drop with decreasing temperature at the temperature, T_m , where the mean kinetic energy of the particles is just sufficient to overcome the SF gap. We obtain T_m as a function of the mass ratio and the interaction strength. The variation of the heat conductivity, at fixed temperature, with the HF potentials and the imbalance chemical potential is also obtained. Finally, because the range of relevant temperatures increases for larger values of the mass ratio, we consider the ${}^6\text{Li}$ - ${}^{40}\text{K}$ mixture separately by taking the temperature dependence of the pair potential into account.

PACS numbers: 03.75.Hh, 03.75.Ss, 68.03.Cd

*Electronic address: n.ebrahimian@aut.ac.ir

†Electronic address: mehrafar@aut.ac.ir

‡Electronic address: afzali@kntu.ac.ir

I. INTRODUCTION

Recently, the study of the behavior of ultracold Fermi gases with two imbalanced hyperfine states has opened up an interesting new area in many-body atomic physics. In this connection, extensive studies have been reported that propose various candidates for the pairing state, including the Fulde-Ferrell-Larkin-Ovchinnikov (FFLO) state [1, 2], the BCS-normal phase separation [3], the Sarma state [4], the p-wave pairing state [5, 6] and the deformed Fermi surface superfluid [7]. Of central importance is the phase separation of a superfluid (SF) paired core surrounded by a polarized normal (N) phase, where, in addition to theoretical studies [8–19], important experimental work has been carried out [20–23]. Such a phase-separation scenario had been proposed by Clogston [24] and Chandrasekhar [25] long ago, who predicted the occurrence of a first-order transition from the N to the SF state. An interesting result in this connection is the appearance of a temperature difference between the two phases as a consequence of the blockage of energy transfer across the N-SF interface. This blockage is due to a SF gap, which causes low-energy normal particles to be reflected from the interface. By studying particle scattering off the interface, the heat conductivity has been calculated [26–28].

In this paper we consider a polarized Fermi system consisting of two spin species with unequal masses in the presence of HF potentials. We concentrate on the BCS regime with various interaction strengths and numerically obtain the allowed values of the chemical and HF potentials, as well as the mass ratio m_r . The functional dependence of the heat conductivity of the N-SF interface on the relevant physical parameters, namely the temperature, the mass ratio, and the interaction strength, is studied in detail. Our focus is on energies slightly above the transmission threshold, because we are considering low temperatures. In our calculations, we therefore use the approximate low-temperature form of the Fermi-Dirac distribution and regard the pair potential as temperature-independent. In particular, we show that the interface conductivity starts to drop with decreasing temperature at the temperature, T_m , where the mean kinetic energy of the particles is just sufficient to overcome the SF gap. The drop is, thus, a result of the blockage of the energy transfer due to the reflection of particles from the interface and signifies a build-up of temperature difference across the interface. We obtain T_m as a function of the mass ratio and the interaction strength. The variation of the heat conductivity, at fixed temperature, with the HF potentials and

the imbalance chemical potential is also obtained. Finally, we single out the particular case of the ${}^6\text{Li}$ - ${}^{40}\text{K}$ mixture ($m_r = 6.7$), due to its importance in experimental and theoretical studies [29–31]. Because the range of relevant temperatures increases for larger values of the mass ratio, here we take the pair potential to be temperature-dependent and use the exact Fermi-Dirac distribution instead of its approximate low-temperature form.

II. HARTREE-FOCK POTENTIAL AND MASS ASYMMETRY EFFECTS

We consider a polarized Fermi gas consisting of two fermionic species (imbalanced hyperfine states \uparrow, \downarrow) of masses m_\uparrow, m_\downarrow and chemical potentials $\mu_\uparrow, \mu_\downarrow$ at sufficiently low temperature. The $\uparrow - \downarrow$ interaction is assumed to be a contact interaction characterized by the coupling constant $V = -4\pi a/m_R$ ($\hbar = 1$) with $m_R = 2m_\uparrow m_\downarrow / (m_\uparrow + m_\downarrow)$. For the superfluid phase we define the species-imbalance chemical potential, $h_s = (\mu_\uparrow - \mu_\downarrow)/2$, and the average chemical potential, $\mu_s = (\mu_\uparrow + \mu_\downarrow)/2 - U_s$, where U_s is the superfluid HF potential. For the calculation of transmission coefficients, and hence the heat conductivity, we need to obtain the solution of Bogoliubov-de Gennes equations [32]. The effective hamiltonian of the system may be written as

$$H = \int d^3x \sum_i [\psi^\dagger(\mathbf{r}i)H(\mathbf{r}i)\psi(\mathbf{r}i) + U(\mathbf{r}i)\psi^\dagger(\mathbf{r}i)\psi(\mathbf{r}i) + \Delta(\mathbf{r})\psi^\dagger(\mathbf{r}\uparrow)\psi^\dagger(\mathbf{r}\downarrow) + \Delta^*(\mathbf{r})\psi(\mathbf{r}\downarrow)\psi(\mathbf{r}\uparrow)] \quad (1)$$

where $H(\mathbf{r}i) = -\frac{\nabla^2}{2m_i} - \mu_i$ ($i = \uparrow, \downarrow$) and

$$U(\mathbf{r}\uparrow) = -V < \psi^\dagger(\mathbf{r}\downarrow)\psi(\mathbf{r}\downarrow) >, \quad U(\mathbf{r}\downarrow) = -V < \psi^\dagger(\mathbf{r}\uparrow)\psi(\mathbf{r}\uparrow) > \\ \Delta(\mathbf{r}) = -V < \psi(\mathbf{r}\downarrow)\psi(\mathbf{r}\uparrow) > = V < \psi(\mathbf{r}\uparrow)\psi(\mathbf{r}\downarrow) >$$

are the HF and pair potentials, respectively. We use the approximation that U and Δ are independent of \mathbf{r} . It is noted that in the superfluid phase (unlike the normal phase) all the HF potentials are equal [33]. The traditional forms of $\psi(\mathbf{r}\uparrow)$ and $\psi(\mathbf{r}\downarrow)$ are

$$\psi(\mathbf{r}\uparrow) = \sum_{\mathbf{k}} (\gamma_{\mathbf{k}\uparrow} u_{\mathbf{k}}(\mathbf{r}\uparrow) - \gamma_{\mathbf{k}\downarrow}^\dagger v_{\mathbf{k}}^*(\mathbf{r}\downarrow)), \quad \psi(\mathbf{r}\downarrow) = \sum_{\mathbf{k}} (\gamma_{\mathbf{k}\downarrow} u_{\mathbf{k}}(\mathbf{r}\downarrow) + \gamma_{\mathbf{k}\uparrow}^\dagger v_{\mathbf{k}}^*(\mathbf{r}\downarrow)) \quad (2)$$

where γ, γ^\dagger (u, v) are the fermionic quasiparticle operators (wavefunctions). By using these expressions and the commutation relations between γ, γ^\dagger and H , one can straightforwardly

obtain the Bogoliubov-de Gennes equations

$$\begin{aligned} [H(\mathbf{r} \uparrow) + U(\uparrow)]u(\mathbf{r} \uparrow) + \Delta v(\mathbf{r} \downarrow) &= Eu(\mathbf{r} \uparrow) \\ \Delta^* u(\mathbf{r} \uparrow) - [H(\mathbf{r} \downarrow) + U(\downarrow)]v(\mathbf{r} \downarrow) &= Ev(\mathbf{r} \downarrow). \end{aligned} \quad (3)$$

One obtains the second set of equations by interchanging \uparrow and \downarrow . In the α -channel, we take $u(\mathbf{r} \uparrow)$ for the particle-like and $v(\mathbf{r} \downarrow)$ for the hole-like wavefunctions.

To proceed, let us take the N-SF interface to be in the $x = 0$ plane and introduce the superscript s (n) for the solutions in the SF (N) phase. We also introduce $\phi_{\mathbf{k}(q)}^\pm(\mathbf{r}) = \exp[i(\mathbf{k}_\parallel \cdot \mathbf{r} \pm k_{(q)}x)]$ for the N phase, and $\phi_{\mathbf{k}}^{\pm(q)}(\mathbf{r}) = \exp[i(\mathbf{k}_\parallel \cdot \mathbf{r} \pm k^{(q)}x)]$ for the SF phase, where $q = p, h$ refers to particle, hole and \mathbf{k}_\parallel ($k^{(q)}, k_{(q)}$) denotes the component of the wave vector \mathbf{k} parallel (perpendicular) to the interface. Notice that q appears as a subscript (superscript) for the N (SF) phase throughout our notation.

From the Bogoliubov-de Gennes equations we obtain the relations, $k_{(h)}^2 = k_{(p)}^2 + 2m_\uparrow[U(\uparrow) - m_r U(\downarrow) + U_s(m_r - 1) - 2\varepsilon]$ and $k^{(p,h)^2} = k_{(p)}^2 + 2m_\uparrow(U(\uparrow) - U_s - \xi^\pm)$, where $m_r = m_\downarrow/m_\uparrow$ (mass ratio), $2\varepsilon = (E + h_s)(1 + m_r) + \mu_s(1 - m_r)$, and $\xi^\pm = \varepsilon \mp \sqrt{\varepsilon^2 - m_r \Delta^2}$. Thus for the N phase we write

$$u_{\mathbf{k}}^{(n)}(\mathbf{r} \uparrow) = \sum_{\sigma=\pm} U_{\mathbf{k}(p)}^\sigma \phi_{\mathbf{k}(p)}^\sigma(\mathbf{r}), \quad v_{\mathbf{k}}^{(n)}(\mathbf{r} \downarrow) = \sum_{\sigma=\pm} V_{\mathbf{k}(h)}^\sigma \phi_{\mathbf{k}(h)}^\sigma(\mathbf{r}). \quad (4)$$

As for the SF phase,

$$u_{\mathbf{k}}^{(s)}(\mathbf{r} \uparrow) = \sum_{q,\sigma} U_{\mathbf{k}}^{\sigma(q)} \phi_{\mathbf{k}}^{\sigma(q)}(\mathbf{r}), \quad v_{\mathbf{k}}^{(s)}(\mathbf{r} \downarrow) = \sum_{q,\sigma} V_{\mathbf{k}}^{\sigma(q)} \phi_{\mathbf{k}}^{\sigma(q)}(\mathbf{r}) \quad (5)$$

where $V_{\mathbf{k}}^{\sigma(p)} = BU_{\mathbf{k}}^{\sigma(p)}$ and $V_{\mathbf{k}}^{\sigma(h)} = B^{-1}U_{\mathbf{k}}^{\sigma(h)}$ with $B = \xi^+/\Delta$. The amplitudes $U_{\mathbf{k}(p)}^\sigma$, etc. are to be determined by matching the wave functions and their derivatives at $x = 0$, of course [34].

Denoting $\xi_{(p)} \equiv k_{(p)}^2/2m_\uparrow$, for $\xi^+ - U(\uparrow) + U_s < \xi_{(p)} < \mu_\uparrow - U(\uparrow) + E$, particle-like and hole-like excitations both occur in the SF side, but Andreev reflection [35] is forbidden. However, for $\mu_\uparrow - U(\uparrow) + E < \xi_{(p)} < 2\varepsilon - U(\uparrow) + m_r U(\downarrow) - U_s(m_r - 1)$, we have particle-like and hole-like excitations, as well as normal and Andreev reflections [27]. In other regions, the particle has insufficient energy to excite the SF side and, thus, the transmission coefficients vanish. We, therefore, restrict our attention to the above two regions, which we shall denote by I and II, respectively. Moreover, our focus is on energies slightly above the transmission threshold ($\varepsilon \approx \sqrt{m_r} \Delta$), because we are considering low temperatures.

Denoting the x -component of the current density by j_x , the transmission coefficient is given by $W = j_x^T / j_x^I$, where the superscripts T and I refer to the transmitted and incident quasi-particle current densities, respectively. The general form of \mathbf{j} (for α -channel) is

$$\begin{aligned} \mathbf{j}_\alpha(\mathbf{r}) = & -\frac{i}{2m_\uparrow} [u^*(\mathbf{r} \uparrow) \nabla u(\mathbf{r} \uparrow) - u(\mathbf{r} \uparrow) \nabla u^*(\mathbf{r} \uparrow)] \\ & -\frac{i}{2m_\downarrow} [-v^*(\mathbf{r} \downarrow) \nabla v(\mathbf{r} \downarrow) + v(\mathbf{r} \downarrow) \nabla v^*(\mathbf{r} \downarrow)]. \end{aligned} \quad (6)$$

The heat conductivity (for α -channel) is given by

$$\kappa = \frac{m_\uparrow}{\pi^2(1+m_r)^2} \frac{\partial}{\partial T} \int \int d\xi_{(p)} d\varepsilon (\varepsilon - \varepsilon_0) f(\varepsilon, T) W(\varepsilon, \xi_{(p)}) + (\uparrow \rightarrow \downarrow, p \rightarrow h) \quad (7)$$

where $\varepsilon_0 = \varepsilon|_{E=0}$ and $f(\varepsilon, T)$ is the Fermi-Dirac distribution, which, in the low temperature limit $T \ll \sqrt{m_r} \Delta$ ($k_B = 1$), reduces to $e^{-T_m/T}$ (up to a proportionality constant), where

$$\frac{3}{2} T_m = 2 \frac{\sqrt{m_r} \Delta - \varepsilon_0}{1 + m_r}. \quad (8)$$

The right hand side is the minimal energy attained by the α spectra, which is positive (in order to have a gapped spectrum) and independent of the HF potentials.

In the mass asymmetric case, analytical calculation of the heat conductivity in the BCS regime (unlike the deep BCS regime in which the Andreev approximation is valid) is a formidable task, especially when HF potentials are present. We, therefore, approach the problem numerically and examine the effect of the HF potentials and mass asymmetry in regions I and II. We begin by obtaining the allowed range of values for all the relevant parameters in the BCS regime. To this end, we use the following standard relations. The HF potential of the superfluid phase, obtained by using the fermionic anticommutation relations for γ and γ^\dagger , is given by the number equation

$$U_s = V n_s = \frac{1}{2} V \int \frac{d^3 k}{(2\pi)^3} \left(1 - \frac{\zeta_{\mathbf{k}}}{\sqrt{\zeta_{\mathbf{k}}^2 + \Delta^2}} \right) \quad (9)$$

where $\zeta_{\mathbf{k}} = \varepsilon_{\mathbf{k}} - \mu_s = \mathbf{k}^2/2m_R - \mu_s$. Similarly, the gap equation is given by

$$1 = \frac{1}{2} V \int \frac{d^3 k}{(2\pi)^3} \left(\frac{1}{\sqrt{\zeta_{\mathbf{k}}^2 + \Delta^2}} - \frac{1}{\varepsilon_{\mathbf{k}}} \right). \quad (10)$$

The above integrals can be calculated using [36]

$$\int_0^\infty dz \frac{z^\lambda}{[(z-1)^2 + x^2]^{1/2}} = -\frac{\pi}{\sin \pi \lambda} (1+x^2)^{\lambda/2} P_\lambda \left(\frac{-1}{\sqrt{1+x^2}} \right) \quad (11)$$

where P_λ is the Legendre function. Equations (9) and (10), thus, yield

$$\frac{1}{m_R a^2} = -\frac{2\mu_s}{\varsigma} P_{1/2}^2(\varsigma), \quad U_s = -\mu_s \left[1 - \frac{P_{3/2}(\varsigma)}{\varsigma P_{1/2}(\varsigma)} \right] \quad (12)$$

where $\varsigma = -[1 + (\Delta/\mu_s)^2]^{-1/2}$. Since $n_s = k_F^3/3\pi^2$, using (12) we find

$$(k_F a)^{-3} = \frac{4}{3\pi} \frac{P_{1/2}^3(\varsigma)}{P_{3/2}(\varsigma) - \varsigma P_{1/2}(\varsigma)}. \quad (13)$$

This relationship determines the allowed values of ς by fixing $1/k_F a$ in the BCS regime. Through (12) we thus find μ_s , U_s , Δ , and the latter yields h_s via the Clogston limit. We, therefore, have μ_\uparrow and μ_\downarrow as well. In the normal phase we similarly find [27]

$$U(\uparrow) = -\frac{4\sqrt{2}m_R a^5}{3\pi} [m_\downarrow(\mu_\downarrow - U(\downarrow))]^{3/2}, \quad U(\downarrow) = -\frac{4\sqrt{2}m_R a^5}{3\pi} [m_\uparrow(\mu_\uparrow - U(\uparrow))]^{3/2} \quad (14)$$

which yield the allowed values of $U(\uparrow)$ and $U(\downarrow)$ in the BCS regime. For m_r less than a cut-off value M (which depends on the interaction strength), we find two solutions for each $U(i)$, satisfying $U_s < U(i) < 0$ (for $m_r > M$, no real solution exists). Since the interactions are attractive the upper bound on the potentials is obvious. The lower bound implies that the density of the SF phase (the core region) exceeds that of the N phase. This reconciles with the fact that a N-SF interface exists, separating an unpolarized SF from a partially polarized N phase. Therefore, we take $1 \leq m_r < M$ for the allowed range of values of m_r in the BCS regime.

III. RESULTS AND DISCUSSION

The relevant physical parameters in a dilute Fermi gas are the temperature, the mass ratio, and the interaction strength. It is, therefore, important to find how physical quantities depend on these parameters [37]. For the heat conductivity, (7) is found to give

$$\frac{\kappa}{\kappa_N} = G\left(\frac{T_F}{T}\right)^{3/2} e^{-\frac{3}{2}\frac{T_m}{T}} \quad (15)$$

where T_m is defined by (8), $\kappa_N = T(\mu_\uparrow m_\uparrow + \mu_\downarrow m_\downarrow)/\pi^2$ is the heat conductivity of the N phase, and T_F is the Fermi temperature. The functional forms of $G(\frac{1}{k_F a}, m_r)$ and $T_m(\frac{1}{k_F a}, m_r)$ will be discussed shortly. We note that, as a consequence of (15), κ/κ_N starts to drop from its maximum value at $T = T_m$ with decreasing temperature. This signifies a build up of

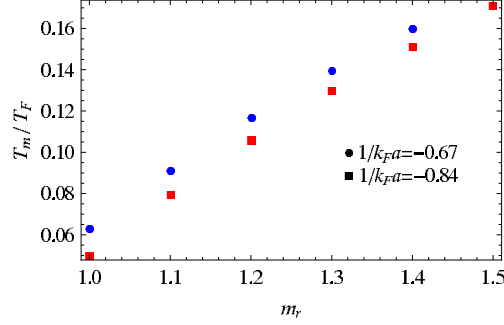


FIG. 1: (Color online) T_m versus m_r .

temperature difference across the interface, which be understood as follows. According to (8), at $T = T_m$, the mean kinetic energy of the particles is just sufficient to overcome the SF gap. We, therefore, expect a blockage of energy transfer at lower temperatures, resulting in the reflection of particles from the interface and hence a drop in the interface conductivity. T_m is an increasing function of m_r , which, for fixed m_r , increases with the interaction strength too (Fig. 1).

Fig. 2 shows typical results for the temperature variation of κ/κ_N using $1/k_F a = -0.84, -0.67$. As seen, for fixed m_r , the larger the absolute value of $1/k_F a$ (i.e., the weaker the interaction), the larger is the heat conductivity. Also, in the presence of HF potentials, the maximum value of κ is almost the same for all m_r for sufficiently weak interactions.

Furthermore, the κ/κ_N at fixed temperature decreases with m_r (Fig. 3), resulting in an increase in the temperature difference across the interface. This means that the characteristic relaxation time increases with m_r . Note that for sufficiently high values of the mass ratio, κ/κ_N is independent of the interaction strength, provided $T/T_F \lesssim 0.03$.

Fig. 4 shows typical curves of κ/κ_N versus T at fixed h_s , for $m_r = 1, 1.4$. At fixed T , κ/κ_N decreases with increasing h_s , because of the growing interaction strength. The effect of h_s (which can be controlled by the species population imbalance) on κ is more pronounced in the presence of HF potentials, because the latter affect the threshold line ($\varepsilon = \Delta\sqrt{m_r}$) by changing ε . However, as seen, the role of h_s diminishes at sufficiently low temperatures.

The functional forms of G and T_m in (15) have been determined by the method of least-squares fit. They are valid for the whole BCS regime and reproduce the above results very accurately:

$$G\left(\frac{1}{k_F a}, m_r\right) = g_0(m_r) + \frac{1}{k_F a} g_1(m_r) + \left(\frac{1}{k_F a}\right)^2 g_2(m_r)$$

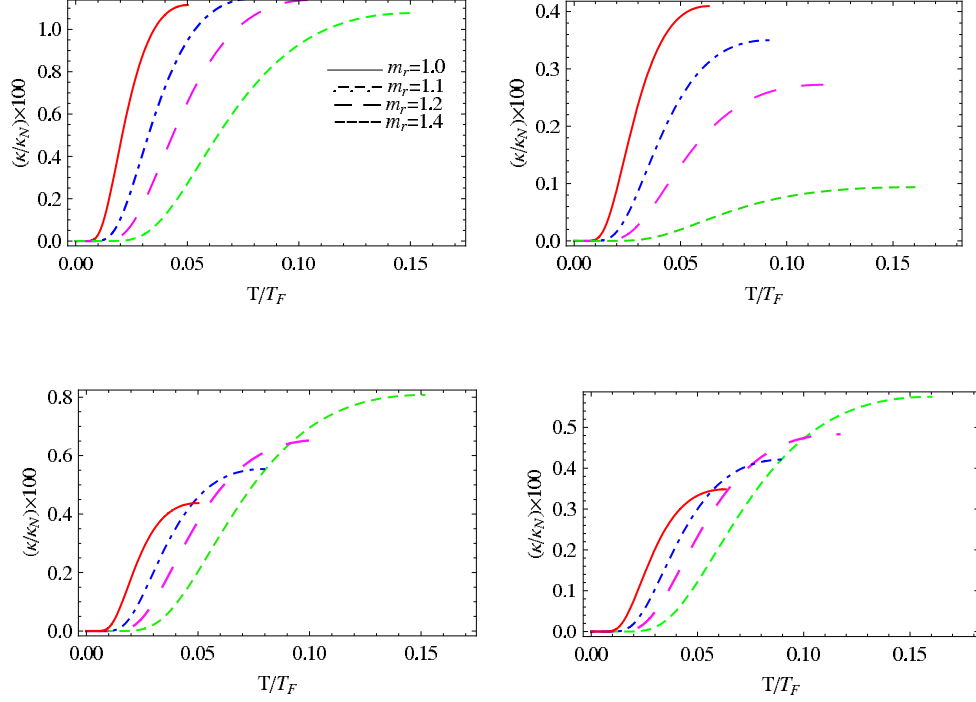


FIG. 2: Interface conductivity versus temperature for $1/k_F a = -0.84$ (left) and -0.67 (right), with (top) and without (bottom) HF potentials.

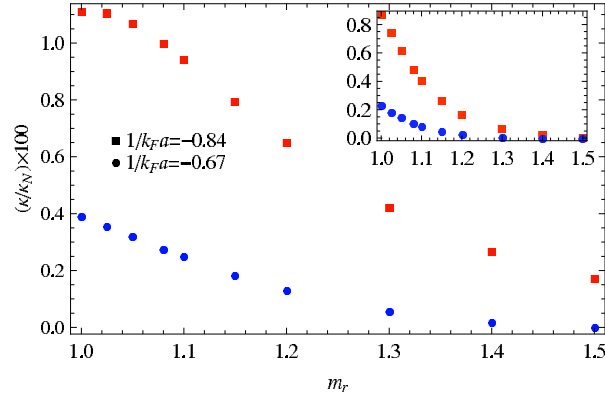


FIG. 3: (Color online) Interface conductivity versus mass ratio at $T/T_F = 0.05$ and 0.03 (inset).

$$\frac{3}{2}T_m\left(\frac{1}{k_F a}, m_r\right) = \frac{T_F m_r}{1 + m_r} \left[t_0(m_r) + \frac{1}{k_F a} t_1(m_r) + \left(\frac{1}{k_F a}\right)^2 t_2(m_r) \right] \quad (16)$$

where

$$g_0 = -0.51 + \frac{0.93}{\sqrt{m_r}} - \frac{0.43}{m_r}, \quad g_1 = -1.00 + \frac{1.78}{\sqrt{m_r}} - \frac{0.79}{m_r}, \quad g_2 = -0.44 + \frac{0.75}{\sqrt{m_r}} - \frac{0.32}{m_r}$$

$$t_0 = 0.16 + \frac{1.38}{\sqrt{m_r}} - \frac{1.14}{m_r}, \quad t_1 = -0.99 + \frac{1.35}{\sqrt{m_r}} + \frac{0.03}{m_r}, \quad t_2 = -0.34 + \frac{0.39}{\sqrt{m_r}} + \frac{0.07}{m_r}.$$

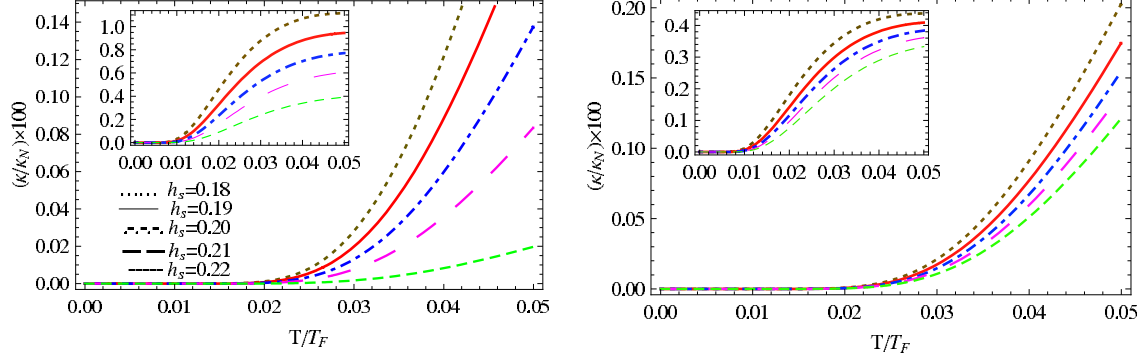


FIG. 4: (Color online) Interface conductivity versus temperature for $m_r = 1$ (inset) and 1.4, with (left) and without (right) HF potentials.

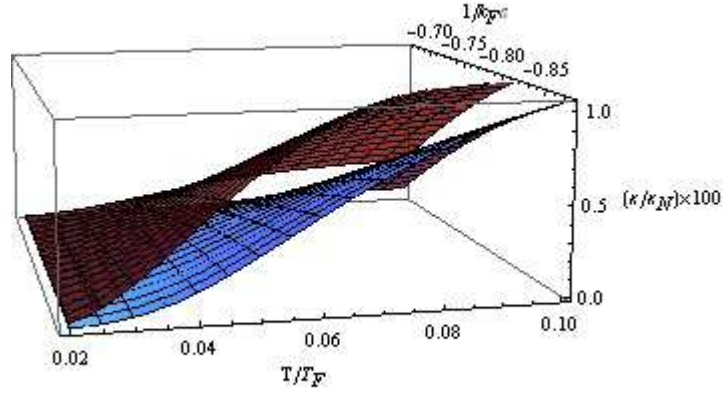


FIG. 5: (Color online) Dependence of interface conductivity on temperature and interaction strength for $m_r = 1.2$ (top) and 1.4 (bottom).

The resulting functional dependence of κ/κ_N on the temperature and interaction strength is depicted in Fig. 5.

The curves of κ/κ_N versus HF potentials at constant temperature are shown in Fig. 6. As seen, the role of the potentials becomes more important as the temperature increases. Also, the heat conductivity decreases with U_\downarrow/U_\uparrow , which is understood because of the resulting increase in the scattering length (and, hence, cross section).

As a subsidiary result, we may also point out that our numerical calculations show that the role of the incident particles (from the N side) with energies in region I (where Andreev reflection does not occur) is much more important in κ than that of the incident

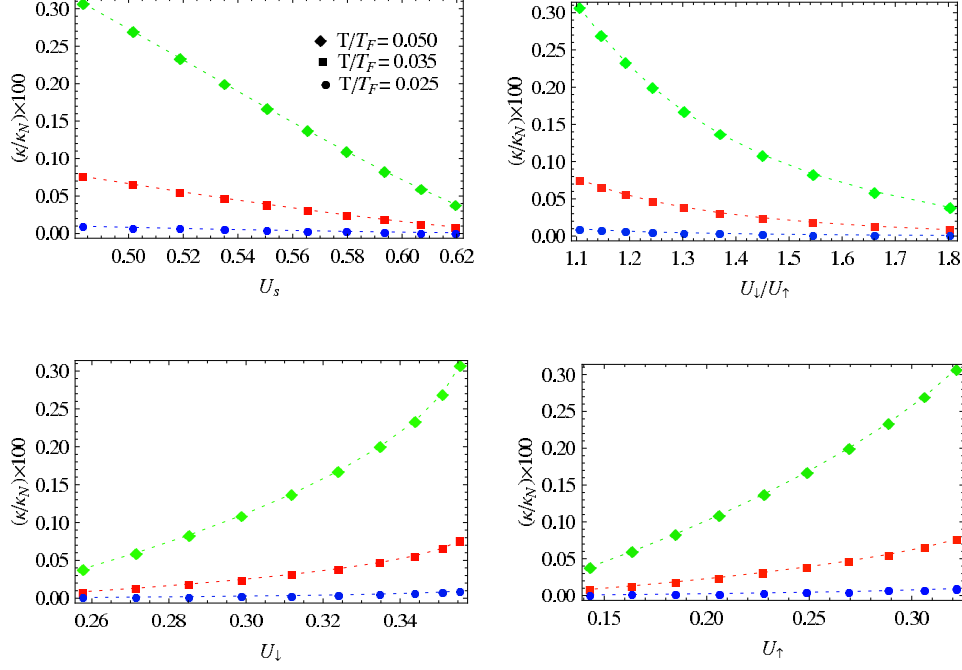


FIG. 6: (Color online) Interface conductivity versus HF potentials for $m_r = 1.4$.

particles/holes with energies in region II.

The mixture ${}^6\text{Li}-{}^{40}\text{K}$

Here, we consider in more detail the particular case of the ${}^6\text{Li}-{}^{40}\text{K}$ mixture ($m_r = 6.7$), due to its importance in experimental and theoretical studies. Since T_m increases with m_r (Fig. 1), for larger values of the mass ratio such as here, the range of relevant temperatures increases. Hence, it would be more appropriate to take the temperature dependence of Δ into account. We have [38]

$$\frac{\Delta(T)}{\Delta} - 1 \propto \left(8 - \frac{T}{\Delta}\right) \sqrt{\frac{T}{\Delta}} e^{-\Delta/T} \quad (17)$$

where Δ is the zero temperature limit considered in our previous calculations. Also, we take the distribution function $f(\varepsilon, T)$ in (7) to be the exact Fermi-Dirac distribution instead of its approximate low-temperature form. (However, for simplicity, we take HF potentials to be zero.)

We find the following analytic expression for the transmission coefficient of region I:

$$W_I = 8(\varepsilon - \varepsilon_0) [2\sqrt{m_r} \Delta(T) (\varepsilon - \sqrt{m_r} \Delta(T))]^{\frac{1}{2}} \times$$

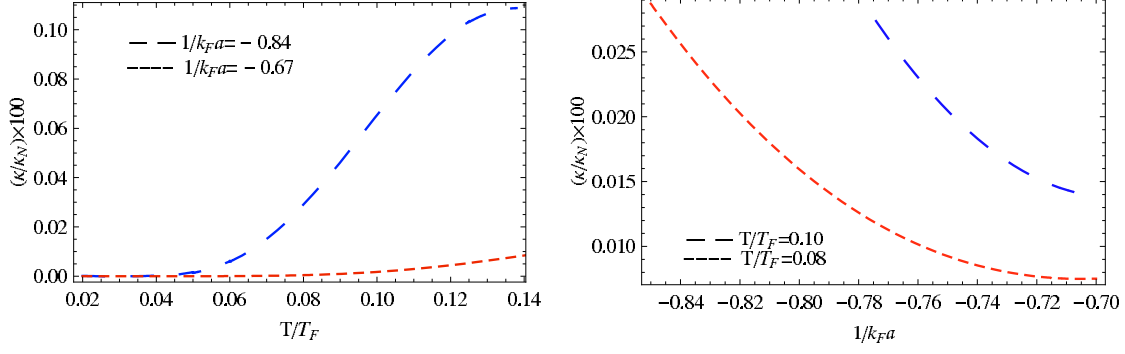


FIG. 7: (Color online) Interface conductivity versus temperature and interaction strength for ${}^6\text{Li}$ - ${}^{40}\text{K}$ mixture.

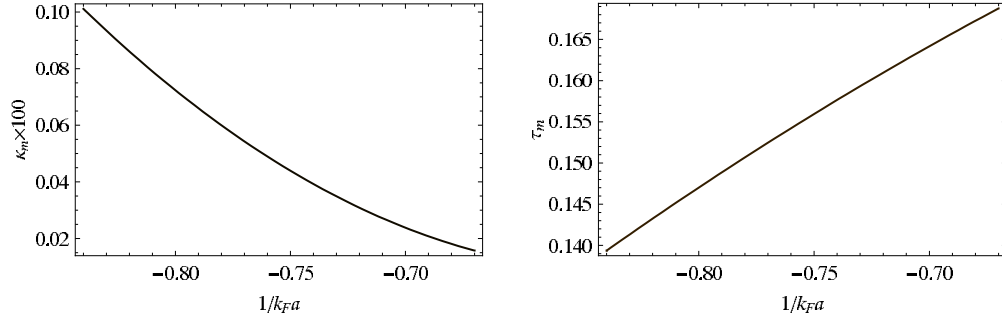


FIG. 8: κ_m and τ_m versus interaction strength for ${}^6\text{Li}$ - ${}^{40}\text{K}$ mixture.

$$\frac{\sqrt{\chi(\chi-1)}[(1+m_r^2)(2\chi-3)+2(m_r^2-1)\sqrt{(\chi-1)(\chi-2)}]}{\left[(m_r-1)+(\sqrt{\chi-2}-\sqrt{\chi})[(m_r-1)\sqrt{\chi}-(m_r+1)\sqrt{\chi-1}]\right]^2} \quad (18)$$

where $\chi = \xi_{(p)}/\Delta(T)\sqrt{m_r}$. By using equations (17), (12), and the definition of ς , we can obtain the temperature dependence of μ_s . The interface conductivity (7) is then obtained via numerical interpolation (Fig. 7). Similarly, the functional forms of κ_m and τ_m (the maximum values of κ/κ_N and T/T_F , respectively) have been determined by the method of least-squares fit. They are

$$\begin{aligned} \kappa_m\left(\frac{1}{k_F a}\right) &= 0.006 + 0.02\frac{1}{k_F a} + 0.02\left(\frac{1}{k_F a}\right)^2 \\ \tau_m\left(\frac{1}{k_F a}\right) &= 0.2 - 0.04\frac{1}{k_F a} - 0.14\left(\frac{1}{k_F a}\right)^2. \end{aligned} \quad (19)$$

Fig. 8 shows the graphs of κ_m and τ_m versus the interaction strength.

It is noteworthy that, since $h_s < \sqrt{m_r}\Delta(T) < \mu_s$, where the second inequality sign is owing to the fact that κ is real, the condition for Clogston limit ($h_s \ll \mu_s$) is satisfied more

stringently as m_r increases.

-
- [1] P. Fulde and R.A. Ferrell, Phys. Rev. A **135**, 550 (1964).
 - [2] A.I. Larkin and Y.N. Ovchinnikov, Sov. Phys. JETP **20**, 762 (1965).
 - [3] P.F. Bedaque, H. Caldas, and G. Rupak, Phys. Rev. Lett. **91**, 247002 (2003).
 - [4] W.V. Liu and F. Wilczek, Phys. Rev. Lett. **90**, 047002 (2003).
 - [5] J. Mur-Petit, A. Polls, and H.-J. Schulze, Phys. Lett. A **290**, 317 (2001).
 - [6] A. Bulgac, M.M. Forbes, and A. Schwenk, Phys. Rev. Lett. **97**, 020402 (2006).
 - [7] H. Muther and A. Sedrakian, Phys. Rev. Lett. **88**, 252503 (2002).
 - [8] T.N. De Silva and E.J. Mueller, Phys. Rev. Lett. **97**, 070402 (2006).
 - [9] Y.-P. Shim, R.A. Duine, and A.H. MacDonald, Phys. Rev. A **74**, 053602 (2006).
 - [10] S.K. Baur, S. Basu, T.N. De Silva, and E.J. Mueller, Phys. Rev. A **79**, 063628 (2009).
 - [11] H. Caldas, Phys. Rev. A **69**, 063602 (2004).
 - [12] J. Carlson and S. Reddy, Phys. Rev. Lett. **95**, 060401 (2005).
 - [13] T. Mizushima, K. Machida, and M. Ichioka, Phys. Rev. Lett. **94**, 060404 (2005).
 - [14] F. Chevy, Phys. Rev. Lett. **96**, 130401 (2006).
 - [15] M. Haque and H.T.C. Stoof, Phys. Rev. A **74**, 011602 (2006).
 - [16] D.T. Son and M.A. Stephanov, Phys. Rev. A **74**, 013614 (2006).
 - [17] C. Lobo, A. Recati, S. Giorgini, and S. Stringari, Phys. Rev. Lett **97**, 200403 (2006).
 - [18] D.E. Sheehy and L. Radzihovsky, Ann. Phys. (NY) **322**, 8 (2007).
 - [19] Z.-J. Ying, M. Cuoco, C. Noce, and H.-Q. Zho, Eur. Phys. J. B **78**, 43 (2010).
 - [20] G.B. Partridge, W. Li, R.I. Kamar, Y.A. Liao, and R.G. Hulet, Science **311**, 503 (2006).
 - [21] M.W. Zwerlein, A. Schirotzek, C.H. Schunck, and W. Ketterle, Science **311**, 492 (2006).
 - [22] Y. Shin, M.W. Zwerlein, C.H. Schunck, A. Schirotzek, and W. Ketterle, Phys. Rev. Lett. **97**, 030401 (2006).
 - [23] G.B. Partridge, W. Li, Y.A. Liao, R.G. Hulet, M. Haque, and H.T.C. Stoof, Phys Rev. Lett. **97**, 190407 (2006).
 - [24] A.M. Clogston, Phys. Rev. Lett. **9**, 266 (1962).
 - [25] B.S. Chandrasekhar, Appl. Phys. Lett. **1**, 7 (1962).
 - [26] B. Van Schaeybroeck and A. Lazarides, Phys. Rev. Lett. **98**, 170402 (2007).

- [27] B. Van Schaeybroeck and A. Lazarides, Phys. Rev. A **79**, 053612 (2009).
- [28] N. Ebrahimian, M. Mehrafarin, and R. Afzali, Physica B **407**, 140 (2012).
- [29] E. Wille et. al., Phys. Rev. Lett. **100**, 053201 (2008).
- [30] K. B. Gubbels, J. E. Baarsma, and H. T. C. Stoof, Phys. Rev. Lett. **103**, 195301 (2009).
- [31] J. E. Baarsma, K. B. Gubbels, and H. T. C. Stoof, Phys. Rev. A **82**, 013624 (2010).
- [32] P.G. de Gennes, Superconductivity of Metals and Alloys (Addison-Wesley, New York, 1966).
- [33] J.B. Ketterson and S.N. Song, Superconductivity (Cambridge University Press, U.K., 1995).
- [34] J. Demers and A. Griffin, Can. J. Phys. **49**, 285 (1971).
- [35] A.F. Andreev, Sov. Phys. JETP **19**, 1288 (1964).
- [36] T. Papenbrock and G.F. Bertsch, Phys. Rev. C **59**, 2052 (1999).
- [37] S. Zhang and A.J. Leggett, Phys. Rev. A **79**, 023601 (2009).
- [38] A.A. Abrikosov, L.P. Gorkov, and I.Y. Dzyaloshinskii, Quantum Field Theoretical Methods in Statistical Physics (Pergamon Press, Oxford, 1965).